ISSN: 3066-7194
Research Article
Novel Journal of Applied Sciences Research

Degradation of Malachite Green by Photocatalysis and Dissociative Adsorption using ZnO and Clinoptilolite

Edgar E. Reyna-Ortega*, & Carlos R. Michel

Department of Physics, CUCEI, Universidad de Guadalajara.Blvd. Marcelino García Barragán 1421 Col. Olímpica, Guadalajara Jal. 44430, México.

***Corresponding author:** Edgar E. Reyna-Ortega, Department of Physics, CUCEI, Universidad de Guadalajara.Blvd. Marcelino García Barragán 1421 Col. Olímpica, Guadalajara Jal. 44430, México.

Submitted: 28 November 2025 **Accepted:** 10 December 2025 **Published:** 31 January 2026

Citation: *Reyna-Ortega, E. E., & Michel, C. R. (2026). Degradation of Malachite Green by Photocatalysis and Dissociative Adsorption using ZnO and Clinoptilolite. Nov Joun of Appl Sci Res, 3(1), 01-06.*

Abstract

Malachite Green (MG) is a dye that has generated controversy due to its possible carcinogenic risks. In this work, the degradation of this compound using different natural and synthetic compounds was studied. Two phenomena occur in this process: photocatalysis and dissociative adsorption. To measure the progress of degradation, UV-Vis spectroscopy was employed. The compounds used were zinc formate (ZF), Ag-doped zinc formate (ZF/Ag) and their corresponding oxides calcined at 600°C, ZnO and Ag-ZnO. In addition to them, a commercial organoaluminosilicate corresponding to the mineral clinoptilolite, with commercial brand Carbura Zea T ®, in its natural form (CTS) and calcined at 400°C (CTC) were used. The compounds were characterized by X-ray diffraction and scanning electron microscopy. The estimation of the optical bandgap energy was carried out by the Tauc method in order to predict their photocatalytic efficiency. Maximum photocatalytic MG degradation of 99.25% was measured in ZnO after 10 min of exposure to UV light.

Keywords: Malachite Green, Photocatalysis, Dissociative Adsorption, Clinoptilolite, ZnO, Ag-ZnO.

Introduction

Nowadays it is not new to admit that environmental problems exist, the anthropological contribution is well known, which has increased since 1750´s [1, 2]. Naturally, pollution affects all living beings, including us. Within different surroundings around living matter, water is greatly affected, where sewage plays a critical role. Among different toxic compounds contained in it, synthetic dyes are globally produced in huge amounts, being also the main constituents of industrial effluents [3, 4].

Malachite green (MG) is a synthetic dye used as fungicide since 1933 [5, 6]. Employed to avoid growth of certain organisms in aquaculture and also used as a dye for numerous purposes like wool, leather, paper, and even for microscopic analysis. Unfortunately, MG has also been found in candies made in India [7]. Although, several countries such as USA, Canada, and some countries of the EU have forbidden its use [8]. Due to its toxicity, and its ability to alter DNA molecules, it is important to reduce, remove or degrade it from wastewater.

Among certain methods for remediation of wastewater, photocatalysis (Ph), which is a light driven method that frequently uses nanomaterials, is a promising method to face environmental threats. Photocatalysis induces the promotion of electrons from valence band to conduction band on the semiconductor surface leaving behind positive holes (h+) [9]. These photoelectrons react with positive holes leading to hydroxyl and peroxyl radicals' production, which can oxidize or even mineralize organic compounds. Diverse semiconductor materials have shown high photocatalytic efficiency as TiO2, Fe2O3, ZnO, and SnO2. However, the overall performance and preference of a semiconductor as a photocatalyst is influenced by numerous factors such as photoactivity, cost and non-toxicicity, etc [10].

ZnO is widely known for having high chemical stability, low toxicity, and its easy preparation, in addition to other attractive factors. It has a great performance in Ph with remarkable degradation of organic pollutants due to production of reactive oxygen species (ROS). Furthermore, it is interesting to mention that

ROS are of interest in other areas because of its anticancer or antibacterial applications [9]. R. Sabouni and H. Gomaa also found an efficient degradation of naproxen, ibuprofen and progesterone, higher to 92%, using ZnO as a photocatalyst [11]. Even though ZnO provides promising results in water remediation, efforts continue to upgrade its photocatalytic activity, through a modulation of its bandgap energy Eg (3.7 eV) and a precise control of its particle size and morphology [9].

This work aims to evaluate the photocatalytic efficiency of several materials in the degradation of MG, with a concentration of 10 mg/L as a reference, under different conditions of UV irradiation. The photocatalysts investigated include zinc formate (ZF), 7 wt% Ag-doped zinc formate (ZF/Ag), and their corresponding oxides, ZnO and Ag-ZnO. A commercial organoaluminosilicate, known as the mineral clinoptilolite, corresponding to Carbura Zea T®, in its natural form (CTS) and its calcined form (CTC), was also examined. It is worth to mention that the latter is used for parasite control in livestock, and is produced in large amounts in México.

In order to estimate the degradation potential of these materials as photocatalysts or compounds that promote dissociative adsorption, the Tauc method was applied to determine the optical bandgap energy of each material. Furthermore, adsorption and photolysis (FT) experiments were conducted to provide a comprehensive understanding of MG degradation under those conditions.

Materials and Methods

Zinc formate was obtained by the coprecipitation method using 0.7 g of zinc nitrate hexahydrate purchased from J.T.Baker and 10 mL of concentrated formic acid (>95%, Golden Bell Reactivos). The reaction between them produced a white suspension, with the emission of a brown gas, presumably NO2. The solvent was then evaporated in a microwave oven at low power. Finally, calcination was performed in a programmable convection oven (Yamato DX402) at 100°C for 8 hours. ZF/Ag was prepared using the same amounts as those used in ZF synthesis, along with 0.05 g of silver nitrate (99.9% J.T.Baker®). The same experimental procedure was used in this case. The Ag doping in ZF/Ag is approximately 7 wt% of ZF. The materials produced in this stage were calcined at 150, 200, 300, 500, and 600°C for 5 hours in a Thermolyne muffle furnace model 49000. Regarding aluminosilicate, the uncalcined form CTS, was previously sieved with a <75 μm mesh. This material was calcined at 400°C for 5 hours and the resulting powder was labeled as CTC. XRD was used for crystal structure analysis using a Panalytical diffractometer (Empyrean) at room temperature, which uses monochromatic Cu Kα1 radiation (λ = 1.5406 Å). Additionally, a Hitachi SEM microscope was used to observe particle size and morphology of samples, which were previously gold-sputtered.

To evaluate MG dye degradation, 40 mL of MG solution (10mg/L) were used mixed with 40 mg of material previously ground in a mortar, using a magnetic stirring plate. For proper incorporation of each candidate in the solution, the mixture was also subjected to ultrasonic homogenization for 30 s. The resulting mixture was placed in a Petri dish, where it was kept stirring until the end of the experiment. Each experiment lasted 3 hours.

Photocatalysis and adsorption experiments were carried out as mentioned before. Additionally, a photolysis experiment was conducted. The UV light source used in light-driven phenomena has a λ = 405 nm produced by a LED diode with constant optical irradiance of 10 mW/cm² at a distance no greater than 5 cm from the Petri dish. The LED diode was mounted behind a heat sink to avoid overheating. The following figure illustrates the components used in photocatalysis experiments.

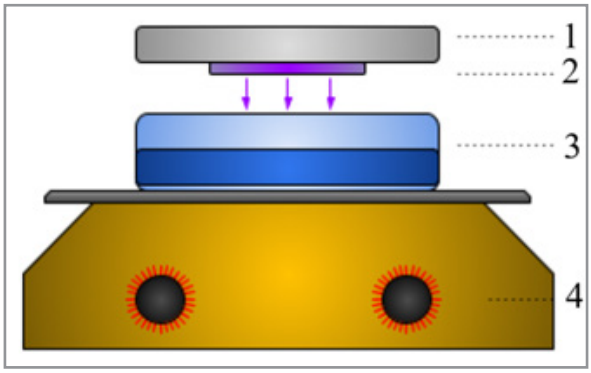

Figure 1: Experimental diagram for photocatalysis experiments. 1: heat sink. 2: UV LED. 3: Petri dish with MG solution and the material used. 4: magnetic stirrer.

The degradation percentage was calculated according to the following expression, from absorbance data obtained by UV-Vis spectroscopy, using a double-beam Helios Zeta spectrophotometer (Thermo Scientific).

$$\%\ Degradation\ (D) = \frac{C_o - C}{C_o} x100\% = \frac{A_o - A}{A_o} x100\% \quad (1)$$

Where C0 corresponds to the initial concentration of the dye solution and C is the concentration of aliquots. A0 and A are the optical absorbance with an analogous meaning. The degradation percentage refers to the decrease in the absorbance band centered at 617 nm. Finally, Lagergren pseudo first-order kinetic and Langmuir-Hinshelwood models were used for fitting adsorption and photocatalysis degradation processes [12]. FT was modeled by a simple linear equation.

Results

Figure 2 displays the crystalline evolution with temperature of the precursor ZF obtained at room temperature. Precursor at 100°C corresponds to an anhydrous phase of zinc formate [13]. Meanwhile, at 150°C a dihydrate zinc formate was identified according to the JCPDS No. 00-014-0761.

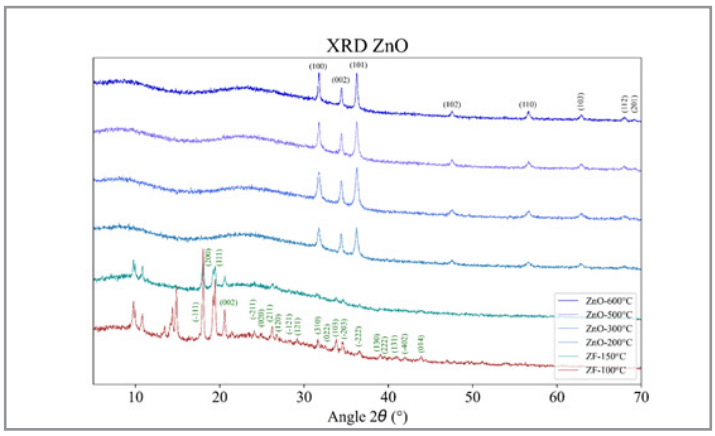

Figure 2: Evolution of diffraction patterns from ZF to ZnO. Miller indices in green correspond to dihydrated ZF, and those in black to ZnO.

According to XRD patterns, from 200 to 600°C, ZnO was identified as the hexagonal-wurtzite phase according to the JCPDS file No. 036-1451, which is the most common and stable phase under ambient conditions [14]. In figure 3, the same previous compounds were identified besides silver, marked in red numbers, according to JCPDS No. 04-0783.

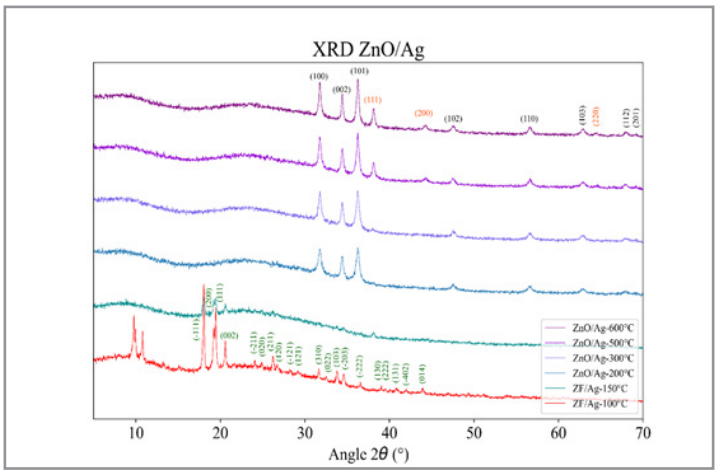

Figure 3: Evolution of diffraction patterns from ZF/Ag to ZnO/Ag. Miller indices in orange correspond to Ag.

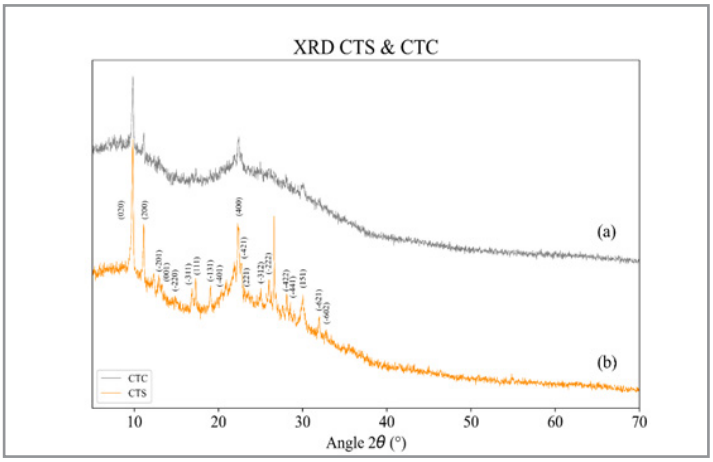

Figure 4: XRD patterns of Carbura Zea T®. (a) calcined (CTC). (b) uncalcined (CTS). Miller indices in black correspond to clinoptilolite.

The diffraction patterns of the organoaluminosilicate are shown in figure 4, with (a) CTC and (b) CTS. Plane indices of clinoptilolite were mainly identified, noting a preferential orientation of the (020) plane compared to (400), according to JCPDS No. 29-1349. At 2θ□26.6° an intense peak is observed, potentially quartz [15]. Furthermore, the presence of other minerals was not assessed due to the great number of similar materials. Clinoptilolite is a natural zeolite used to remove toxins and heavy like lead, mercury, cadmium and chromium, from water, but also it is also used in animal nutrition. Other applications are found in fertilizers, and as an additive in glass fabrication and in the manufacture of paper and cardboard. The XRD pattern of CTS, shown in figure 4, revealed that most peaks vanished as temperature increases compared to the as-received product. As it will be

shown later, specifically at 400°C CTS improved its adsorption properties, losing around 14% of its weight due to dehydration and dehydroxylation [16].

The morphology observed by SEM from samples ZnO and Ag-ZnO is shown in figure 5, where (a) corresponds to ZnO and (b) to Ag-ZnO. Both samples show particles of irregular shape and size in the nanometer scale. The particle size in Ag-ZnO is more homogeneous than in ZnO, with extensive particle agglomeration throughout the samples.

Table 1 shows the estimated bandgap energies of the target materials. Due to the narrower Eg values the best candidates for photocatalysis were ZnO and Ag-ZnO, with very large values obtained for the zeolite samples and formates.

Table 1: Optical bandgap (E_g) energies of samples calculated by the Tauc technique

Material	CTC	CTS	Ag-ZnO	ZnO
E_g (eV)	4.62–5.37	5.17–5.58	3.7–3.9	3.69–3.79

Regarding the degradation of MG solutions, figure 6 shows adsorption vs. time graphs obtained from ZnO, Ag-ZnO and CTC samples, which were performed in the dark. In this figure, the solid lines correspond to an exponential fitting. The R2 values calculated by using the OriginLab software from each graph are shown in the inset. As expected, the better degradation results were obtained from ZnO and Ag-ZnO samples, but considering the low cost and great abundance of CTC, the result obtained from it of approximately 68% after 20 min represents a suitable and attractive option for this application.

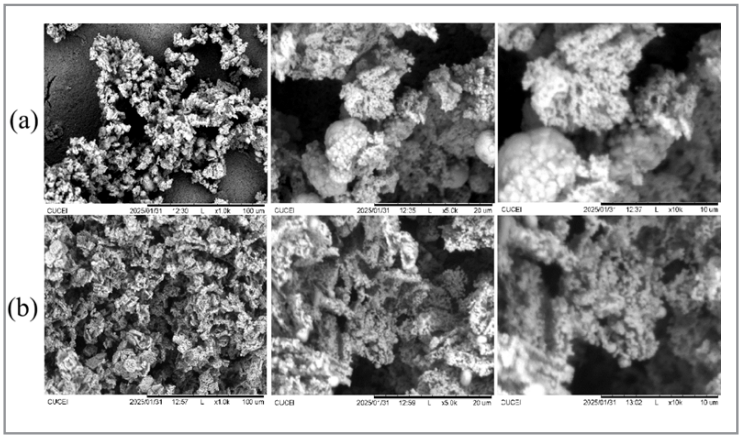

Figure 5: Morphology of the samples observed by SEM. (a) ZnO calcined at 600 °C. (b) ZnO/Ag calcined at 600 °C. For each material, images at 1000×, 5000×, and 10000× magnification are shown from left to right.

Table 1. Optical bandgap (E_g) energies of samples calculated by the Tauc technique

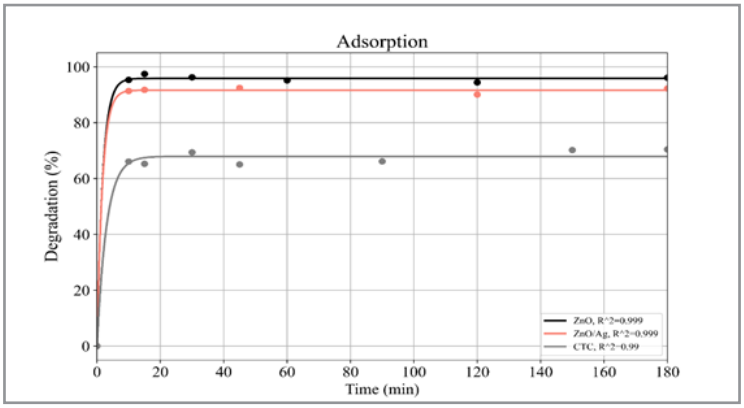

Figure 6: Percentage of MG degradation by the photocatalysis method. The Lagergren pseudo–first-order kinetic model was employed for curve fitting

Regarding the results obtained from photocatalysis, figure 7 shows the corresponding curves, as well as that collected from a photolysis (FT) experiment. It is important to note that while the Ph experiments are being carried out, photolysis and dissociative adsorption occur simultaneously, and even when the adsorption phenomenon is expected to take place solely, photolysis also occurs. Therefore, photocatalysis results are produced by a combination of phenomena. According to the results shown in Figure 6, the adsorption of MG using the oxides and CTC remained practically constant along the experiment, and it occurs very rapidly. Since certain variations in the degradation percentage can be observed in curves in figure 7, traces of suspended material with MG dye adsorbed may be present during the extraction of samples, with a continuous effect during their storage.

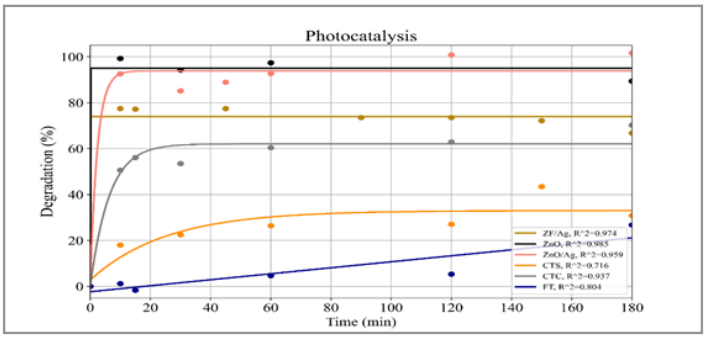

Figure 7: Percentage of MG degradation by the adsorption method. Langmuir–Hinshelwood model was employed for curve fitting.

Discussion

A remarkable feature observed in MG degradation graphs is that it starts in the first minutes, with a sharp increase, indicating that MG degradation was incredibly fast. These results contrasted with those registered from other samples, where the degradation was significantly slower. Moreover, as can be seen in figures 6 and 7, when UV light was used in ZnO and ZnO/Ag experiments the results were similar in terms of curve fitting. However, ZnO was more efficient in the first 10 minutes, reaching 99.25% of MG degradation, outperforming all the compounds, as it was expected.

Table 2 summarizes the degradation percentages for those results above 50%. From figure 6, and all mentioned in the previous paragraph, the compounds where the greatest change was observed were CTS and ZF/Ag. In the absence of UV light, the valence band electrons do not have sufficient energy to reach the conduction band and eventually form ROS, making them able to perform dye degradation through adsorption processes. For these materials, the Ph method showed a significant improvement in degrading MG compared to adsorption. Particularly notable is the significant change observed in ZF when doped with approximately 7 wt% of silver.

Table 2: Percentage of degradation for MG dye at 10 min

Material	Method	Degradation (%)
ZnO	Ph	99.25
ZnO	Adsorption	95.35
ZnO/Ag	Ph	92.57
ZnO/Ag	Adsorption	91.35
ZF/Ag	Ph	77.44
CTC	Adsorption	66.08

The degradation by adsorption can be associated to different causes, such as the pH of the solution, the exposure time between the catalyst and the dye, the temperature of the mixture, etc. In a synthesis of flower-shaped ZnO nanoparticles, Kataria and Garg stated that the ZnO surface becomes positive for pH < 4 and negative for pH > 4 [17]. This pH value is known as the point of zero charge. There is electrostatic repulsion between the MG molecules and ZnO, resulting in lower degradation [18]. Under this context, the pH of the solution must have promoted the degradation of MG, specifically in the oxides.

Conclusion

The highest MG degradations using Ph and adsorption were exhibited by ZnO and ZnO/Ag (7 wt% Ag) respectively, and as expected by lowest optical bandgap energy for ZnO. Although MG dye degradation is similar for ZnO and ZnO/Ag in both methods, a short UV exposure period for large water volumes is more economical, highlighting 7 wt% Ag-doped ZnO was not as effective as using ZnO.

Although zeolite materials such as the mineral clinoptilolite, having an optical bandgap energy greater than 4 eV did not exhibit a comparable dye degradation than ZnO, conducted experiments suggests that these materials represent an important alternative for water treatment at a very low cost and great efficiency, which no previous reference found in the literature.

Acknowledgments

Authors thank the Universidad de Guadalajara for financial support and all facilities that made this work possible.

References

1. Andres, R. J., Fielding, D. J., Marland, G., Boden, T. A., Kumar, N., & Kearney, A. T. (2016). Carbon dioxide emissions from fossil-fuel use, 1751–1950. Tellus B: Chemical and Physical Meteorology, 51(4), 759–765.
2. Yoro, K., & Daramola, M. (2020). CO_2 emission sources, greenhouse gases, and the global warming effect. In Advances in carbon capture (pp. 1–28).
3. Liu, H., Guo, W., Li, Y., He, S., & He, C. (2018). Photocatalytic degradation of sixteen organic dyes by TiO_2/WO_3-coated magnetic nanoparticles under simulated visible light and solar light. Journal of Environmental Chemical Engineering, 6(1), 59–67.
4. Khataee, A. R., & Kasiri, M. B. (2010). Photocatalytic degradation of organic dyes in the presence of nanostructured titanium dioxide: Influence of the chemical structure of dyes. Journal of Molecular Catalysis A: Chemical, 328(1), 8–26.
5. Cooksey, C. (2016). Quirks of dye nomenclature. 6. Mala-

chite green. Biotechnic & Histochemistry, 91(6), 438–444.
6. EFSA Panel on Contaminants in the Food Chain (CONTAM). (2016). Malachite green in food. EFSA Journal, 14(7), e04530.
7. Hidayah, N., Abu Bakar, F., Mahyudin, N. A., Faridah, S., Nur-Azura, M. S., & Zaman, M. Z. (2013). Detection of malachite green and leuco-malachite green in fishery industry. International Food Research Journal, 20, 1511–1519.
8. Fakhri, Y., Mahmoudizeh, A., Hemmati, F., Adiban, M., Esfandiari, Z., & Mousavi Khaneghah, A. (2025). The concentration of malachite green in fish: A systematic review, meta-analysis, and probabilistic risk assessment. International Journal of Environmental Health Research, 35, 2651–2666.
9. Sun, Y., Zhang, W., Li, Q., Liu, H., & Wang, X. (2023). Preparations and applications of zinc oxide based photocatalytic materials. Advanced Sensor and Energy Materials, 2(3), 100069.
10. Gouasmia, A., Zouaoui, E., Mekkaoui, A. A., Haddad, A., & Bousba, D. (2022). Highly efficient photocatalytic degradation of malachite green dye over copper oxide and copper cobaltite photocatalysts under solar or microwave irradiation. Inorganic Chemistry Communications, 145, 110066.
11. Sabouni, R., & Gomaa, H. (2019). Photocatalytic degradation of pharmaceutical micro-pollutants using ZnO. Environmental Science and Pollution Research, 26, 5372–5380.
12. Michel, C., & Martínez-Preciado, A. (2022). Photocatalytic performance of β-Ga_2O_3 microcubes towards efficient degradation of malachite green. Ceramics International, 48(7), 9746–9752.
13. Arii, T., Kishi, A., & Kobayashi, Y. (1998). A new simultaneous apparatus for X-ray diffractometry and differential scanning calorimetry (XRD–DSC). Thermochimica Acta, 325(2), 151–156.
14. Shaba, E. Y., Jacob, J., Tijani, J., & Suleiman, M. (2021). A critical review of synthesis parameters affecting the properties of zinc oxide nanoparticles and their application in wastewater treatment. Applied Water Science, 11, 48.
15. Jamo, H. U. (2016). Structural analysis and surface morphology of quartz. Bayero Journal of Pure and Applied Sciences, 9(2), 230–233.
16. Mansouri, N., Rikhtegar, N., Panahi, H., Atabi, F., & Karimi Shahraki, B. (2013). Porosity, characterization and structural properties of natural zeolite—clinoptilolite—as a sorbent. Environmental Protection Engineering, 39(1), 139–152.
17. Kataria, N., & Garg, V. K. (2017). Removal of Congo red and brilliant green dyes from aqueous solution using flower shaped ZnO nanoparticles. Journal of Environmental Chemical Engineering, 5(6), 5420–5428.
18. Idriss, H., & Alakhras, A. (2020). Clean up of malachite green dye in aqueous solution using ZnO nanopowder. Journal of Optoelectronics and Biomedical Materials, 12(4), 109–119.